

Persistent photoconductivity in $\text{In}_x\text{Al}_y\text{Ga}_{1-x-y}\text{N}$ quaternary alloys

C. H. Chen, D. R. Hang, W. H. Chen, Y. F. Chen, H. X. Jiang, and J. Y. Lin

Citation: *Applied Physics Letters* **82**, 1884 (2003); doi: 10.1063/1.1558959

View online: <http://dx.doi.org/10.1063/1.1558959>

View Table of Contents: <http://scitation.aip.org/content/aip/journal/apl/82/12?ver=pdfcov>

Published by the [AIP Publishing](#)

Articles you may be interested in

[Mechanism of enhanced luminescence in \$\text{In}_x\text{Al}_y\text{Ga}_{1-x-y}\text{N}\$ quaternary alloys](#)

Appl. Phys. Lett. **80**, 1397 (2002); 10.1063/1.1455147

[Growth and optical properties of \$\text{In}_x\text{Al}_y\text{Ga}_{1-x-y}\text{N}\$ quaternary alloys](#)

Appl. Phys. Lett. **78**, 61 (2001); 10.1063/1.1331087

[Photoresponsivity of ultraviolet detectors based on \$\text{In}_x\text{Al}_y\text{Ga}_{1-x-y}\text{N}\$ quaternary alloys](#)

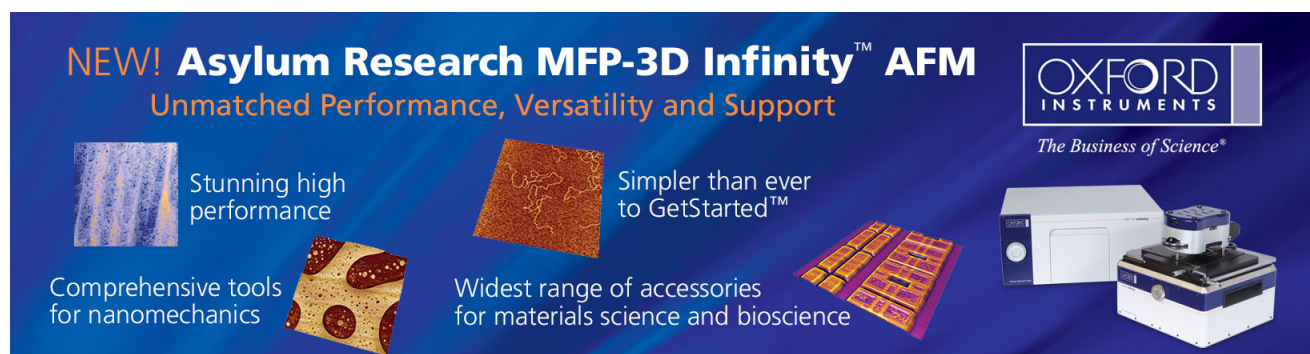
Appl. Phys. Lett. **77**, 791 (2000); 10.1063/1.1306540

[Positive and negative persistent photoconductivities in semimetallic \$\text{Al}_x\text{Ga}_{1-x}\text{Sb}/\text{InAs}\$ quantum wells](#)

J. Appl. Phys. **86**, 3152 (1999); 10.1063/1.371182

[Theoretical and experimental studies in n-type modulation-doped \$\text{In}_x\text{Ga}_{1-x}\text{As}/\text{In}_y\text{Al}_{1-y}\text{As}/\text{InP}\$ magnetic sensors](#)

J. Appl. Phys. **86**, 1535 (1999); 10.1063/1.370926

The advertisement features a dark blue background with white and orange text. At the top left, it reads 'NEW! Asylum Research MFP-3D Infinity™ AFM' in large white letters, followed by 'Unmatched Performance, Versatility and Support' in orange. To the right is the Oxford Instruments logo, which includes the text 'OXFORD INSTRUMENTS' and 'The Business of Science®'. Below the main text are four images: a textured surface, a circular pattern, a grid of small squares, and the AFM instrument itself. Each image is accompanied by a short text description: 'Stunning high performance', 'Simpler than ever to GetStarted™', 'Comprehensive tools for nanomechanics', and 'Widest range of accessories for materials science and bioscience'.

Persistent photoconductivity in $\text{In}_x\text{Al}_y\text{Ga}_{1-x-y}\text{N}$ quaternary alloys

C. H. Chen, D. R. Hang, W. H. Chen, and Y. F. Chen^{a)}

Department of Physics, National Taiwan University, Taipei, Taiwan, Republic of China

H. X. Jiang and J. Y. Lin

Department of Physics, Kansas State University, Manhattan, Kansas 6506-2601

(Received 25 October 2002; accepted 15 January 2003)

The optical properties of $\text{In}_x\text{Al}_y\text{Ga}_{1-x-y}\text{N}$ quaternary alloys were investigated by photoconductivity (PC), persistent photoconductivity (PPC), photoluminescence (PL), and photoluminescence excitation (PLE) measurements. Quite interestingly, persistent photoconductivity was observed. Through the combination of our optical studies, we show that the PPC effect arises from composition fluctuations in $\text{In}_x\text{Al}_y\text{Ga}_{1-x-y}\text{N}$ quaternary alloys. From the analysis of the decay kinetics, the localization depth caused by composition fluctuations was determined. A comparison between the PL, PLE, and PC measurements gives a direct access to the Stokes' shift. The Stokes' shift can be explained in terms of localization due to the existence of nanoscale clusters, and it is consistent with the PPC result. The results shown here provide concrete evidence to support our previously proposed model that the existence of InGaN-like clusters is responsible for the strong luminescence in $\text{In}_x\text{Al}_y\text{Ga}_{1-x-y}\text{N}$ quaternary alloys. © 2003 American Institute of Physics.
[DOI: 10.1063/1.1558959]

The group III-nitride wide-band-gap semiconductors have been recognized as very important materials for many optoelectronic devices, such as blue ultraviolet (UV) light emitting diodes (LEDs), laser diodes (LDs), and high-temperature/high-power electronic devices.¹⁻³ It has been demonstrated that most nitride based devices must take advantage of multiple quantum wells (MQWs) and heterostructures such as GaN/AlGaN (Refs. 4 and 5) and InGaN/GaN (Ref. 6) as well as the tunability of the band gaps in the alloys. Recently, $\text{In}_x\text{Al}_y\text{Ga}_{1-x-y}\text{N}$ quaternary alloys have also been recognized to have the potential to overcome some shortfall of GaN epilayers, InGaN, and AlGaN alloys.¹⁻⁶ By varying In and Al compositions x and y in $\text{In}_x\text{Al}_y\text{Ga}_{1-x-y}\text{N}$, one can change the energy band gap while keeping the lattice matched with GaN, which can be used to reduce dislocation density as well as piezoelectric field. In addition $\text{In}_x\text{Al}_y\text{Ga}_{1-x-y}\text{N}$ quaternary alloys also have the potential to provide a better thermal match to GaN, which could be an important advantage in epitaxial growth. The potential application of $\text{In}_x\text{Al}_y\text{Ga}_{1-x-y}\text{N}$ quaternary alloys as InGaN/InAlGaN quantum well light emitters,⁷ GaN/InAlGaN heterojunction field-effect transistors,⁸ and UV detectors have been demonstrated recently.⁹ It is also found that the quantum efficiency (QE) of $\text{In}_x\text{Al}_y\text{Ga}_{1-x-y}\text{N}$ is enhanced significantly over AlGaN with a comparable Al content.⁹ The enhanced luminescent efficiency has been attributed to the existence of alloy clusters.¹⁰ In this letter, we report the observation of the persistent photoconductivity (PPC) effect in $\text{In}_x\text{Al}_y\text{Ga}_{1-x-y}\text{N}$ quaternary alloys. We point out that the PPC effect is caused by potential fluctuations in $\text{In}_x\text{Al}_y\text{Ga}_{1-x-y}\text{N}$ quaternary alloys. In order to obtain the depth of potential fluctuations, the observed PPC effect was investigated with focus on its decay kinetics at different temperature. Together with the studies on photoconductivity

(PC), photoluminescence (PL), photoluminescence excitation (PLE) spectra, and our previous results,¹⁰ we show that potential fluctuations in $\text{In}_x\text{Al}_y\text{Ga}_{1-x-y}\text{N}$ quaternary alloys arise from the existence of InGaN-like clusters.

A set of $\text{In}_x\text{Al}_y\text{Ga}_{1-x-y}\text{N}$ quaternary alloys with different Al concentration has been grown by metalorganic chemical vapor deposition (MOCVD). A 1.0 μm GaN epilayer was first deposited on the sapphire substrate with 25 nm low temperature GaN buffer layer, followed by the deposition of 0.1 μm $\text{In}_x\text{Al}_y\text{Ga}_{1-x-y}\text{N}$ quaternary alloy epilayer by the low pressure metalorganic chemical vapor deposition (MOCVD). The growth temperature and pressure for the lower GaN epilayer were 1050 °C and 300 Torr, respectively. For $\text{In}_x\text{Al}_y\text{Ga}_{1-x-y}\text{N}$ quaternary alloys, the growth temperature 780 °C and In and Al compositions were controlled by varying the flow rates of TMIIn and TMAI. Contents of In and Al were determined by different methods including x-ray diffraction (XRD), energy dispersive system, and Rutherford backscattering.⁹ It was found that $\text{In}_x\text{Al}_y\text{Ga}_{1-x-y}\text{N}$ quaternary alloys, which are lattice matched with GaN epilayers ($y \sim 4.8x$, which is very close to the theoretical value), have the highest PL intensity as well as the narrowest XRD line-width. For the lattice-match sample studied here, the composition is $x=0.026$, $y=0.124$, and for the lattice-mismatch sample $x=0.026$, $y=0.3$. For the PL measurement, the sample was excited by a He-Cd laser working at 325 nm, dispersed by a Spex 0.85 m double-grating spectrometer, and the spectra was detected by a photomultiplier tube. Similar arrangements were used for the PLE measurement except the dispersed light from the Xe lamp was used as the continuous radiation. For the PC measurements, ohmic contacts were formed by depositing indium drops to the four corners of the sample and annealing the sample at 400 °C for 10 s. A Xe lamp was used as the light source, which was dispersed by a 0.27 m monochromator. A constant direct voltage was applied and the conductivity was measured by Keithley 2400 source measure unit. Details of PPC measurement procedure

^{a)}Electronic mail: yfchen@phys.ntu.edu.tw

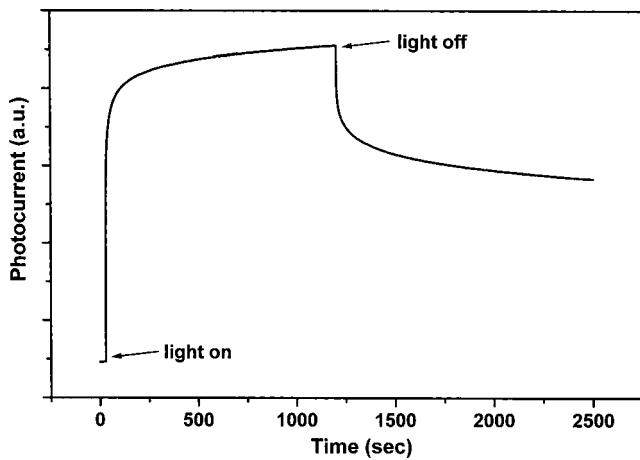


FIG. 1. Typical buildup and decay behavior of PPC in $\text{In}_x\text{Al}_y\text{Ga}_{1-x-y}\text{N}$ lattice-matched sample at 11 K.

were similar to those described previously.¹¹ All the data obtained under different conditions were taken in such a way that the system was always allowed to relax to equilibrium.

Figure 1 shows the photocurrent as a function of time and illumination in lattice-match sample with monochromatic radiation at a photon energy of 3.6 eV taken at 11 K. A strong persistent photoconductivity effect is clearly observed, and similar retention behavior was seen when other monochromatic light with photon energy up to 3.81 eV was used as the illumination source. This PPC effect can be easily understood in terms of the layer alloy potential fluctuations, resulting from the existence of nanoscale clusters in $\text{In}_x\text{Al}_y\text{Ga}_{1-x-y}\text{N}$ quaternary alloys, such as InGaN-like clusters discussed in our previous report.¹⁰ At low temperature, the photoexcited electrons and holes are trapped and separated by local potential fluctuations, the recombination of electron-hole pairs is inhibited, and hence, PPC occurs. The PPC decay curves of lattice-match and lattice-mismatch samples are shown in Fig. 2. For comparison, each curve is normalized to unit at the time when illumination is switched off. We see that the PPC decays slower for the lattice-match sample. Probably, it is due to the fact that the lattice-match sample has smaller defect density, and the remaining carriers can have a longer lifetime.

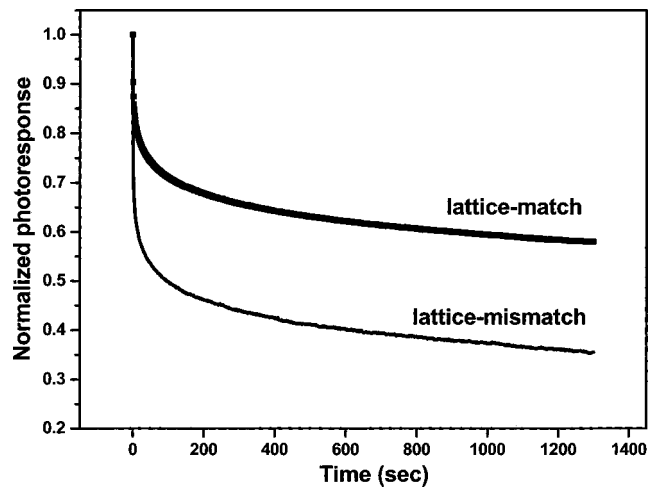


FIG. 2. Photoconductivity decay curves for different Al content at 11 K. Each curve is normalized to unity at $t=0$, the moment when the pumping light is off.

The decay kinetics in photocurrent after turning off the illumination shows a stretched-exponential behavior that can be formulated as¹²

$$I_{\text{ppc}}(t) = I_{\text{ppc}}(0) \exp[-(t/\tau)^\beta], \quad (0 < \beta < 1), \quad (1)$$

where $I_{\text{ppc}}(0)$ is the PPC buildup level at the moment of light excitation being removed, τ is the PPC decay time constant and β is the decay exponent. Figure 3 shows a representative plot of $\ln\{\ln[I_{\text{ppc}}(0)] - \ln[I_{\text{ppc}}(t)]\}$ vs $\ln(t)$ for the lattice-match sample at 11 K. The good linear behavior of the plot demonstrates that PPC decay can be well described by Eq. (1). The stretched-exponential relaxation has been commonly observed in disordered systems¹² and implies that the origin of the observed PPC effect has the similar property. A least-squares fit to the experimental data yields a time constant $\tau \sim 3 \times 10^4$ s, which is much longer than that of the lattice-mismatch sample used here (the obtained decay time constant is about 1×10^3 s for the lattice-mismatch sample).

It is worth noting that the PPC effect can be observed up to room temperature. To obtain the average depth of potential fluctuations, we have performed the measurements at different temperatures. It shows two distinct temperature regions.

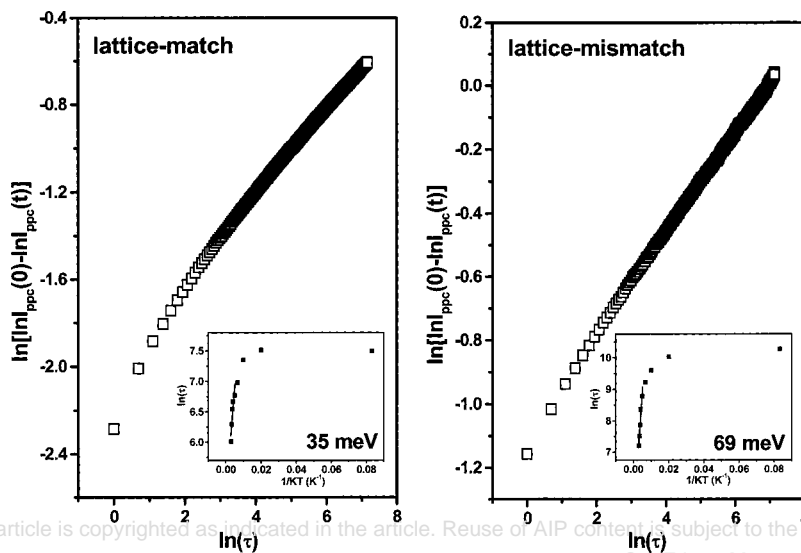


FIG. 3. Plot of $\ln\{\ln[I_{\text{ppc}}(0)] - \ln[I_{\text{ppc}}(t)]\}$ vs $\ln(t)$ for $\text{In}_x\text{Al}_y\text{Ga}_{1-x-y}\text{N}$ lattice match and mismatch samples at 11 K. The linear curve indicate that PPC decays according to stretched-exponential function $I_{\text{ppc}} = I_{\text{ppc}}(0) \exp[-(t/\tau)^\beta]$. The inset shows the capture barrier ΔE obtained according to $\tau = \tau_0 \exp(\Delta E/kT)$.

At low temperature, τ is weakly dependent on temperature. This behavior can be understood as follows. The photoexcited electrons are spatially separated in local potential minima. In order to have an efficient recombination, the trapped electrons and holes have to overcome a potential barrier. At low temperature, there is not enough energy to activate carriers into extended states, the recombination is thus caused by carrier hopping between localized states. The PPC decay is due to wave function overlap between electrons and holes through the process of quantum tunneling, which does not depend on temperature. At high temperature, the probability of thermal activation of the localized carriers to overcome the potential barrier increases with increasing temperature. The PPC decay rate therefore rapidly increases with increasing temperature. In the thermal activation region, this carrier capture barrier ΔE , which characterizes the energy difference between the localized states and the flat band edge, can be estimated from the temperature dependence of the time constant, τ :

$$\tau = \tau_0 \exp(\Delta E / \kappa T). \quad (2)$$

It is found that ΔE is about 69 meV for the lattice-match sample and 35 meV for the lattice-mismatch sample as shown in the inset of Fig. 3. We thus found that the depth of localization is deeper for the lattice-match sample. The different extents of localization can be attributed to the smaller quantum confinement effect of the larger cluster size in lattice-match sample.

According to our studies here, a Stokes' shift with magnitude comparable with ΔE can be expected. In order to confirm this prediction for $\text{In}_x\text{Al}_y\text{Ga}_{1-x-y}\text{N}$ quaternary alloys, we have performed the PL, PLE, and PC measurements. Figure 4 summarizes the PL, PLE, and PC spectra for the lattice-mismatch sample at 15 K. The PL spectrum is dominated by a sharp emission at 3.672 eV and the full width at half maximum (FWHM) is about 40 meV. The lower emission peak at 3.483 eV is due to the lower GaN epilayer. The PLE measurements for the lattice-mismatch sample were monitored at 3.42 eV. We took a multi-Gaussian fit of PLE line and found that the PLE spectrum shows transitions that appear at about 3.485 and 3.71 eV, which are due to the emission of the underneath GaN epilayer and $\text{In}_x\text{Al}_y\text{Ga}_{1-x-y}\text{N}$ layer, respectively. The PC spectral response also shows two component bands, and their superposition results in the measured figure. After the comparison, the emission of the $\text{In}_x\text{Al}_y\text{Ga}_{1-x-y}\text{N}$ quaternary alloy shows a Stokes' shift of 38 meV in magnitude with respect to the absorption edge as determined by PLE spectrum. This value of Stokes' shift is close to the ΔE value discussed above. We also found that the depth of localized states obtained from PPC effect for the lattice-match sample is consistent with the Stokes' shift measured by PL and PLE spectra. Therefore, our results clearly indicate the existence of localized states. We believe the localized states are caused by alloy potential fluctuations in $\text{In}_x\text{Al}_y\text{Ga}_{1-x-y}\text{N}$ quaternary alloys. The origin of potential fluctuations can be attributed to the formation of InGaN-like clusters as discussed in our previous report.¹⁰

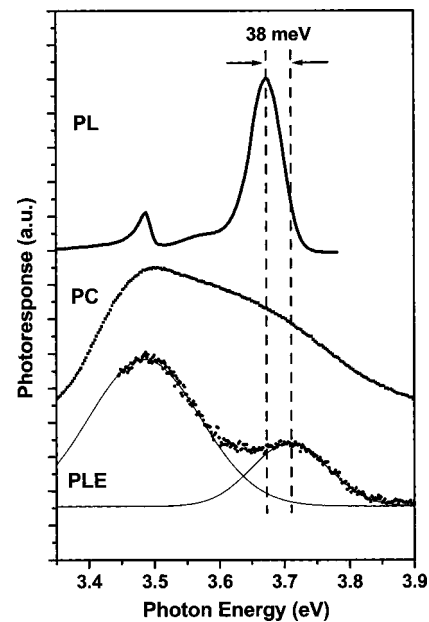


FIG. 4. PL, PLE, and PC spectra of $\text{In}_x\text{Al}_y\text{Ga}_{1-x-y}\text{N}$ lattice-mismatch sample taken at 15 K. The PLE spectrum was fitted by Gaussian curves (solid line). The Stokes' shift is 38 meV between the PL and PLE spectra.

In summary, we discovered the existence of PPC effect in $\text{In}_x\text{Al}_y\text{Ga}_{1-x-y}\text{N}$ quaternary alloys. The decay kinetics of the PPC effect has been investigated from which, the depth of the localization caused by composition fluctuations in $\text{In}_x\text{Al}_y\text{Ga}_{1-x-y}\text{N}$ quaternary alloys is determined. We have also performed PL, PLE, and PC measurements which give a direct access to the Stokes' shift. The obtained Stokes' shift is consistent with the localization depth determined from the PPC result. Our results therefore provide a concrete evidence to support the previously proposed model that the existence of clusters in $\text{In}_x\text{Al}_y\text{Ga}_{1-x-y}\text{N}$ quaternary alloys is responsible for its strong luminescent efficiency.

This work was supported by the Ministry of Education and National Science Council of the Republic of China.

- ¹M. A. Khan, A. Bhattarai, J. N. Kuznia, and D. T. Olson, *Appl. Phys. Lett.* **63**, 1214 (1993).
- ²H. Morkoç, S. Strite, G. B. Gao, M. E. Lin, B. Sverdlov, and M. Burns, *J. Appl. Phys.* **76**, 1363 (1994).
- ³S. Nakamura, M. Senoh, S. Nagahama, N. Iwasa, T. Yamada, T. Matsushita, H. Kiyoko, and Y. Sugimoto, *Jpn. J. Appl. Phys., Part 2* **35**, L74 (1996).
- ⁴C. H. Chen, Y. F. Chen, A. Shih, S. C. Chen, and H. X. Jiang, *Appl. Phys. Lett.* **78**, 3035 (2001).
- ⁵D. R. Hang, C. H. Chen, Y. F. Chen, H. X. Jiang, and J. Y. Lin, *J. Appl. Phys.* **90**, 1887 (2001).
- ⁶H. C. Yang, P. F. Kuo, T. Y. Lin, and Y. F. Chen, K. H. Chen, L. C. Chen, and J.-I. Chyi, *Appl. Phys. Lett.* **76**, 3712 (2000).
- ⁷M. E. Aumer, S. F. LeBoeut, S. M. Bedair, M. Smith, J. Y. Lin, and H. X. Jiang, *Appl. Phys. Lett.* **77**, 821 (2000).
- ⁸M. A. Khan, J. W. Yang, G. Simin, R. Gaska, M. S. Shur, G. Tamulaitis, A. Zukauskas, D. J. Smith, D. Chandrasekhar, and R. Bicknell-Tassius, *Appl. Phys. Lett.* **76**, 1161 (2000).
- ⁹J. Li, K. B. Nam, K. H. Kim, J. Y. Lin, and H. X. Jiang, *Appl. Phys. Lett.* **78**, 61 (2001).
- ¹⁰C. H. Chen, L. Y. Huang, Y. F. Chen, H. X. Jiang, and J. Y. Lin, *Appl. Phys. Lett.* **80**, 1397 (2002).
- ¹¹D. R. Hang, Y. F. Chen, F. F. Fang, and W. I. Wang, *Phys. Rev. B* **60**, 13318 (1999).
- ¹²Y. F. Chen, S. F. Huang, and W. S. Chen, *Phys. Rev. B* **44**, 12748 (1991).